

ADVANCED MATERIALS TECHNOLOGIES

Supporting Information

for *Adv. Mater. Technol.*, DOI 10.1002/admt.202300719

A Tri-Droplet Liquid Structure for Highly Efficient Intracellular Delivery in Primary Mammalian Cells Using Digital Microfluidics

*Samuel R. Little, Ziuwin Leung, Angela B.V. Quach, Alison Hirukawa, Fatemeh Gholizadeh, Mehri Hajiaghayi, Peter J. Darlington and Steve C.C. Shih**

Supporting Information

A tri-droplet liquid structure for highly efficient intracellular delivery in primary mammalian cells using digital microfluidics

Samuel R. Little*,^{1,2} Ziuwin Leung*,^{1,2} Angela Quach,² Alison Hirukawa,³ Fatemeh Gholizadeh,⁴ Mehri Hajiaghayi,⁴ Peter John Darlington,^{4,5} Steve C.C. Shih^{§1,2,4}

¹Department of Electrical and Computer Engineering, Concordia University, Montréal, Québec, Canada

²Centre for Applied Synthetic Biology, Concordia University, Montréal, Québec, Canada

³DropGenie, Boston, Massachusetts, USA

⁴Department of Biology, Concordia University, Montréal, Québec, Canada

⁵PERFORM Center, Department of Health, Kinesiology and Applied Physiology, Concordia University, Montreal, Québec, Canada

*Both authors contributed equally

[§]Corresponding Author – steve.shih@concordia.ca

Table of Contents

Table S1: Electroporation parameters, cell densities, and required concentrations used for different cell lines and payloads	- 3 -
Table S2: Electroporation buffer conductivities and relative permittivity.....	- 4 -
Table S3: Recipes for various custom buffers.	- 4 -
Table S4: payload sequence.....	- 5 -
Figure S1: System overview	- 6 -
Figure S2: triDrop merge and pH change	- 7 -
Figure S3: Buffer vs EP	- 8 -
Figure S4: COMSOL overview	- 9 -
Figure S5: Numerical simulations of various EP buffers.....	- 10 -
Figure S6: Overview of coplanar DMF electroporation designs	- 11 -
Figure S7: Current generation.....	- 12 -
Figure S8: HeLa and Jurkat optimization	- 13 -
Figure S9: Brightfield and GFP images for immortalized cell lines.....	- 14 -
Figure S10: Primary T optimization	- 15 -
Figure S11: Comparison with other recent work – Primary T cell mRNA transfection.....	- 16 -
Figure S12: 5-plex device on-chip operation.....	- 17 -
Figure S13: multi-gRNA vs single gRNA analysis	- 18 -
Figure S14: eGFP plasmid map	- 19 -
Figure S15: Fabrication overview.....	- 20 -
Figure S16: T cell isolation from whole blood	- 21 -
Figure S17: Flow cytometry gating workflow.....	- 22 -

Table S1: Electroporation parameters, cell densities, and required concentrations used for different cell lines and payloads

Cell type	Payloads	Concentration	Pulse Number	Pulse Duration	Cell density (cells/ml)	Voltage (V)	Electric field (kV/cm)
HEK293	70kDa FITC-Dextran	1.2 $\mu\text{g} / \mu\text{L}$	3	10 ms	2x10 ⁷	225	0.57
	250kDa FITC-Dextran						
	2000kDa FITC-Dextran						
	5 kb eGFP-plasmid	51 ng / μL			4x10 ⁷		
HeLa	70kDa FITC-Dextran	1.2 $\mu\text{g} / \mu\text{L}$	3	10 ms	2x10 ⁷	350	0.88
	250kDa FITC-Dextran						
	2000kDa FITC-Dextran				4x10 ⁷		
	5 kb eGFP-plasmid	51 ng / μL					
Jurkat	70kDa FITC-Dextran	1.2 $\mu\text{g} / \mu\text{L}$	3	5 ms	4x10 ⁷	350	0.88
	250kDa FITC-Dextran						
	2000kDa FITC-Dextran						
	1 kb eGFP-mRNA	0.08 $\mu\text{g} / \mu\text{L}$					

	5 kb eGFP-plasmid	51 ng / μ L					
	Cas9 RNP	2 pmol / μ L					
Primary T cells	2000kDa FITC-Dextran	1.2 μ g / μ L	3	3 ms	4×10^7	450	1.13
	5 kb eGFP-plasmid	51 ng / μ L					
	1 kb eGFP-mRNA	0.08 μ g / μ L					
	Cas9 RNP	2 pmol / μ L					

Table S2: Electroporation buffer conductivities and relative permittivity.

Material	Characteristics	
	Electrical conductivity (mS/cm)	Relative permittivity
BTXpress	17.7	80
PBS	16	80
Type R buffer	15.6	80
Type T buffer	8.4	80
ISM(m) buffer	7.5	80
Very high conductive solution	32.0	80

Table S3: Recipes for various custom buffers.

Buffer	Composition
1SM-Modified	5 mM KCl, 15 mM MgCl ₂ .6H ₂ O, 25 mM Sodium succinate, 25 mM Mannitol, pH 7.2
Very high conductive solution	120 mM NaCl, 2.8 mM KCl, 2 mM MgCl ₂ , 20 mM CaCl ₂ , 10 mM HEPES, 11 mM glucose, pH 7.2 with NaOH, 300 mOsm
FACs Buffer	1x PBS, 1 mM EDTA, 25 mM HEPES (pH 7.0), 1% FBS

Table S4: payload sequence

mRNA sequence	AUGGUGAGCAAGGGCGAGGAGCUGUUCACCGGGGUGGUGCCCAUCCU GGUCGAGCUGGACGGCGACGUAAACGGCCACAAGUUCAGCGUGUCCG GCGAGGGCGAGGGGCGAUGCCACCUACGGCAAGCUGACCCUGAAGUUC AUCUGCACCACCGGCAAGCUGCCCUGCCCUGGCCACCCUCGUGACC ACCCUGACCUACGGCGUGCAGUGCUUCAGCCGCUACCCCGACCACAUG AAGCAGCACGACUUCUUAAGUCCGCCAUGCCC GAAGGCUACGUCCA GGAGCGCACCAUCUUCUUAAGGACGACGGCAACUACAAGACCCGCG CCGAGGUGAAGUUCGAGGGGCGACACCCUGGUGAACC GCAUCGAGCUG AAGGGCAUCGACUUAAGGAGGACGGCAACAUC CUGGGGCAACAAGCU GGAGUACAACUACAACAGCCACAACGUCUAUAUCAUGGCCGACAAGC AGAAGAACGGCAUCAAGGUGAACUUAAGAUC CGCCACAACAUCGAG GACGGCAGCGUGCAGCUCGCCGACCACUACCAGCAGAACACCCCAUC GGCGACGGCCCCGUGCUGCUGCCC GACAACCACUACCUGAGCACCCAG UCCGCCUGAGCAAAGACCCCAACGAGAAGCGCGAUCACAUGGUCCU GCUGGAGUUCGUGACCGCCGCGGGGAUCACUCUCGGCAUGGACGAGC UGUACAAGUAA
β2M gRNA	ACUCACGCUGGAUAGCCUCC
TRAC gRNA 1	GUCAGGUUCUGGAUAUCUG
TRAC gRNA 2	GCUGGUACACGGCAGGGUCA
TRAC gRNA 3	CUCUCAGCUGGUACACGGCA
TRAC gRNA 4	UCUCUCAGCUGGUACACGGC

Figure S1: System overview

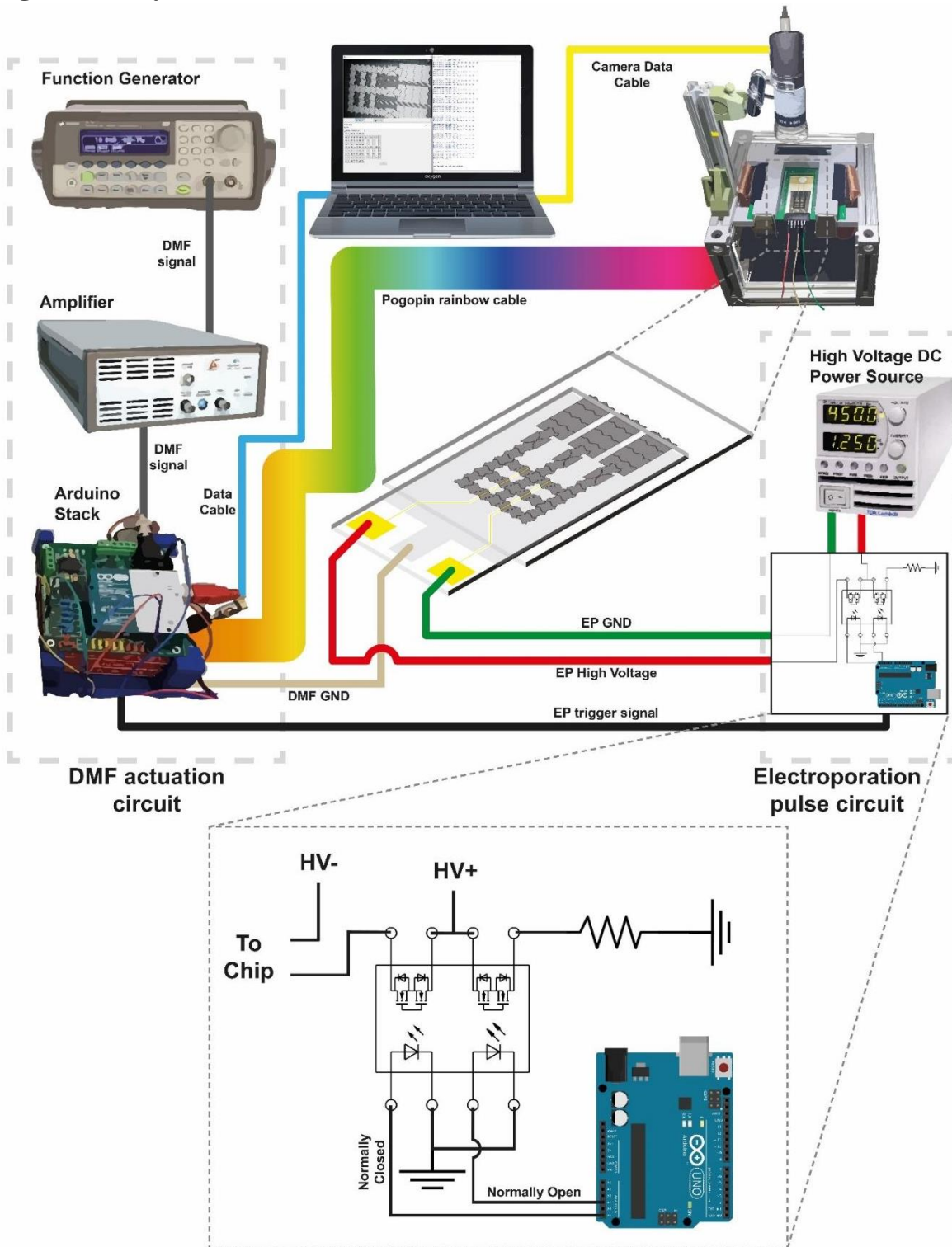


Figure S1: Schematic overview of the complete triDrop automation setup detailing the DMF actuation hardware, automated electroporation pulse generation circuit, and chip holder.

Figure S2: triDrop merge and pH change

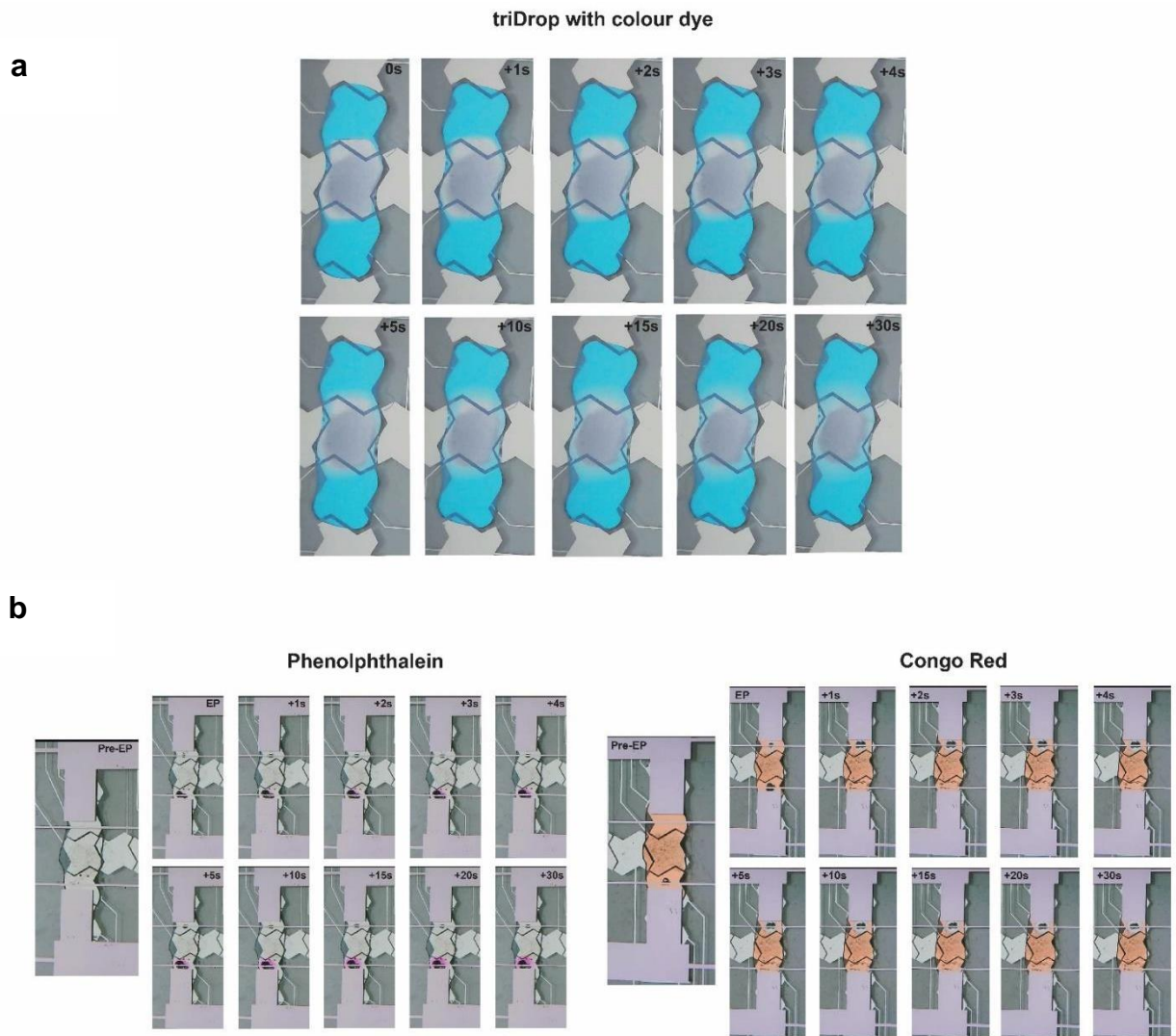


Figure S2: Qualitative assessment of droplet movement on the triDrop system. (a) A triDrop merge operation performed using a standard bottom plate and a transparent Indium Tin Oxide top plate to help visualize liquid mixing. The outer droplets are comprised of high conductive media with 0.05% Pluronic F68 surfactant along with blue dye. The middle droplet is comprised of low conductive media with 0.05% Pluronic F68 surfactant and 4×10^7 cells/mL. Droplets are mixed using standard techniques and left to mix via diffusion for 30 s. (b) A triDrop electroporation procedure using a modified top plate allowing for visualization of the triDrop structure. All three droplets are either doped with phenolphthalein (pH indicator turning purple in the presence of pH above 8.5, left image set), or Congo red (pH indicator turning from red to blue at pH below 5.2, right image set). Three, 200 V_{DC}, 10 ms pulses are applied and the structure was observed for 30 s. The time stamp for each image is shown on the image.

Figure S3: Buffer vs EP

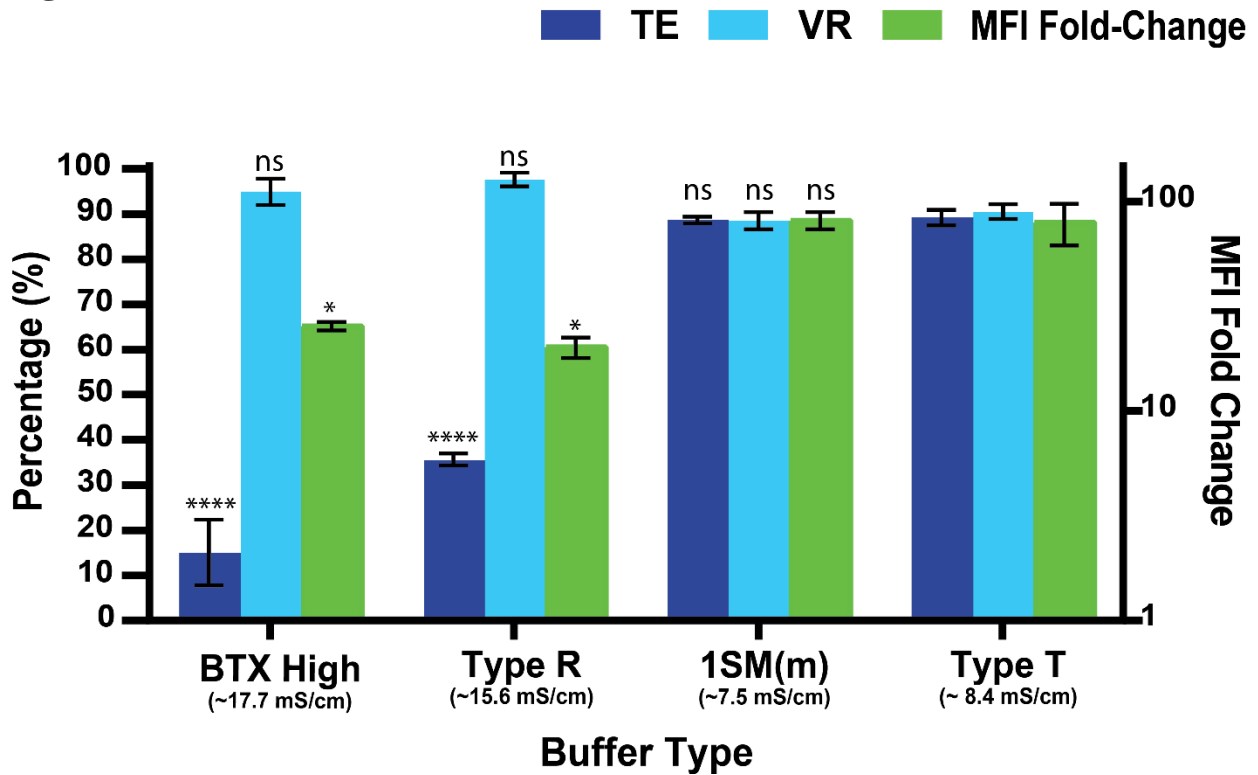


Figure S3: Bar graph comparing triDrop electroporation to insert 70kDa FITC-tagged dextran into HEK293 cells using four different electroporation buffers to form the middle droplet. For each condition three 200 V_{DC} pulses, 10 ms in duration were applied. The outer droplets were comprised of high conductivity media and the middle droplets had cells at 2×10^7 cells/mL. SEM are calculated based of $n = 3$. n.s indicated no significant difference, *, and **** represents P-values below 0.05, and 0.0001 respectively. Statistical analysis was performed using an ordinary one-way ANOVA.

Figure S4: COMSOL overview

Numerical simulations were performed using COMSOL Multiphysics software on a 3D structure. The 3D model of the triDrop structure was generated by taking a video of the triDrop merge sequence using PBS with colored dye as flanking buffers and using a transparent ITO top plate to help visualize the droplets and clearly see the boundaries between the flanking droplets and the sample droplet. The video was analyzed frame by frame and a digital image of the top-down view of the triDrop merge geometry was isolated at 2-seconds post-merge. The image was imported into AutoCAD and the boundaries of the individual droplets were traced to create a model of the triDrop structure. The AutoCAD file was imported into COMSOL Multiphysics and extruded to a final height of 180 μm (the gap between our top and bottom layer). The 3D COMSOL model, illustrated in the **Figure below**, was used in the simulations using a FINE mesh. Using the electric currents physics module, the following equations were used starting with the point form of *Ohm's law*:

$$\mathbf{J} = \sigma\mathbf{E} + \mathbf{J}_e$$

where \mathbf{J} is the current density (SI unit: A/m^2), \mathbf{J}_e is the externally generated current density (SI unit: A/m^2), σ is the electrical conductivity (SI unit: S/m), and \mathbf{E} is the electric field (V/m). Converting this to its continuity then states

$$\nabla \cdot \mathbf{J} = -\nabla \cdot (\sigma \nabla V - \mathbf{J}_e) = 0$$

As such, we can then solve for the scalar electric potential V which can then be used to calculate the electric field \mathbf{E} . The material characteristics for each droplet is listed in **SI Table 2**. The initial conditions and boundaries used for solving the above model are as follows:

1. Temperature = 293.15 K
2. High voltage electroperoration = 200 V
3. Ground potential and initial potential $V = 0$ V

where the high voltage and ground potential were set to the boundaries highlighted in yellow in the Figure below. Using these parameters, a stationary study was used to solve for the electric field \mathbf{E} and **Figure S5 and S6** shows the simulated EF within the triDrop structure of different electroperoration buffers with different conductivities.

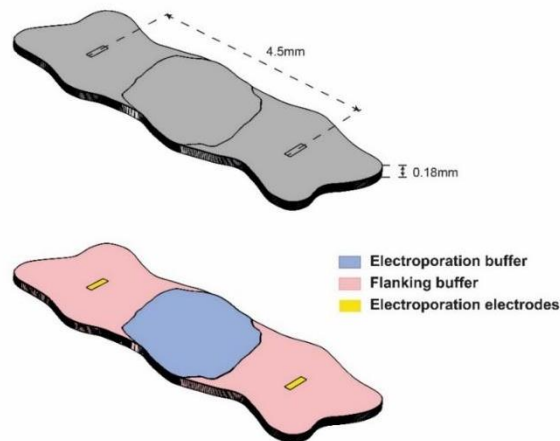


Figure S5: Numerical simulations of various EP buffers

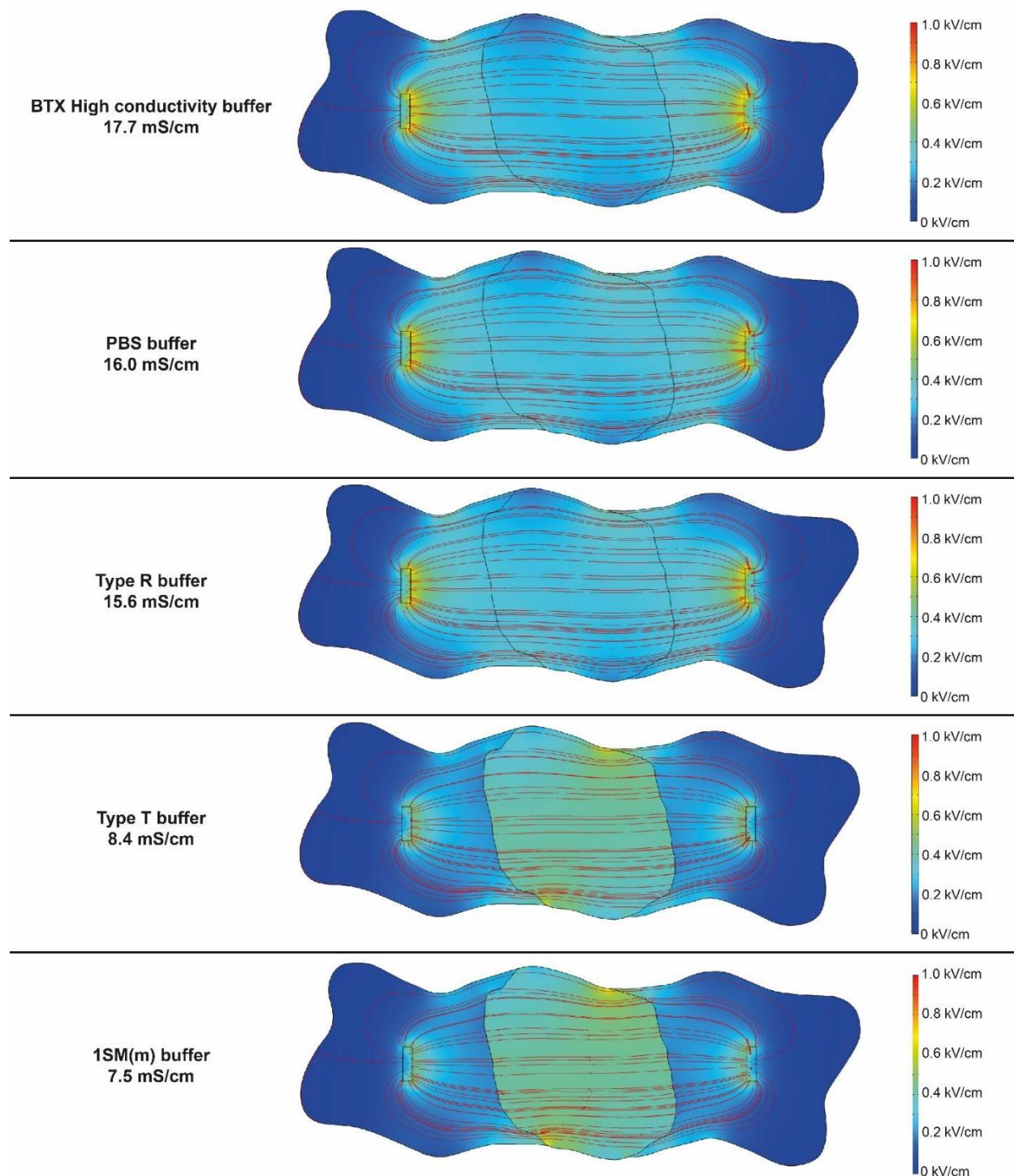
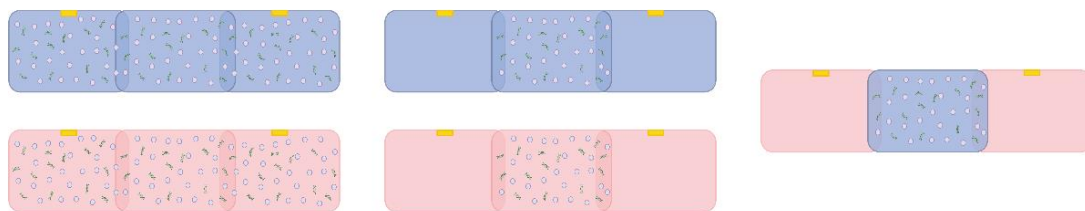


Figure S5: COMSOL simulations showing the electric field generated inside of a triDrop structure when forming the middle droplet out of buffers with different conductivities.

Figure S6: Overview of coplanar DMF electroporation designs

a

■ - High conductivity buffer ■ - Low conductivity buffer ● - Mammalian cell  - Target delivery molecule

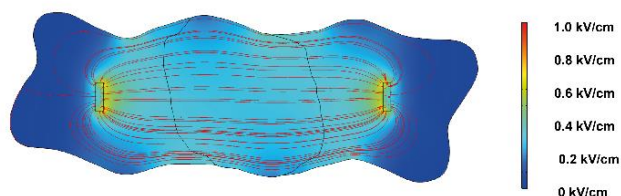


Uniform structure

Focused structure

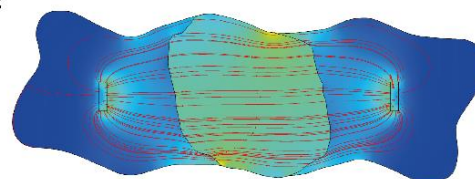
triDrop

b



Uniform/Focused structure

c



triDrop structure

Figure S6: (a) Schematic representation of the 3 different electroporation structures investigated for effective DMF electroporation. (b) COMSOL simulations of the droplet structures when applying a 200V pulse.

Figure S7: Current generation

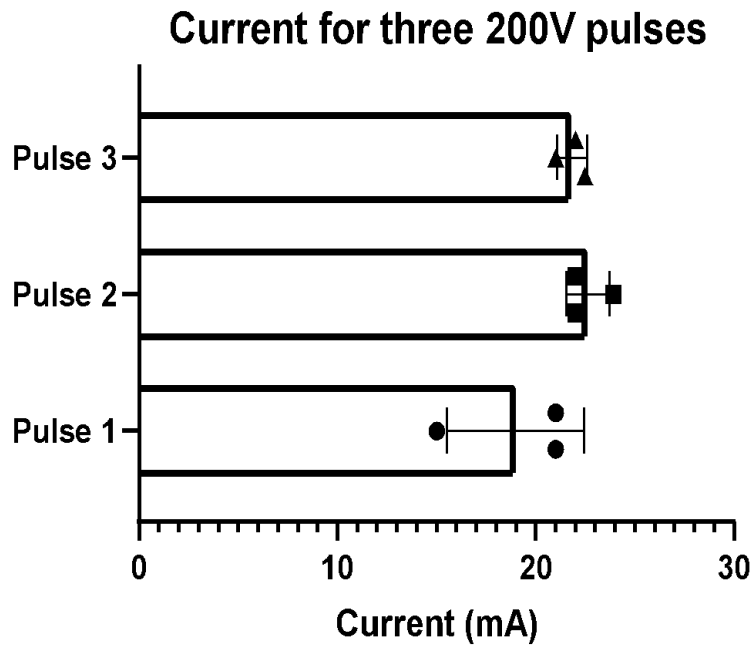


Figure S7: Current measurements for all three pulses during a standard triDrop electroporation process. Three, 200 V_{DC} pulses, 10 ms in duration were applied to a triDrop structure containing 2×10^7 cells/mL. Error bars are based on standard error of the mean for $n = 3$ replicates.

Figure S8: HeLa and Jurkat optimization

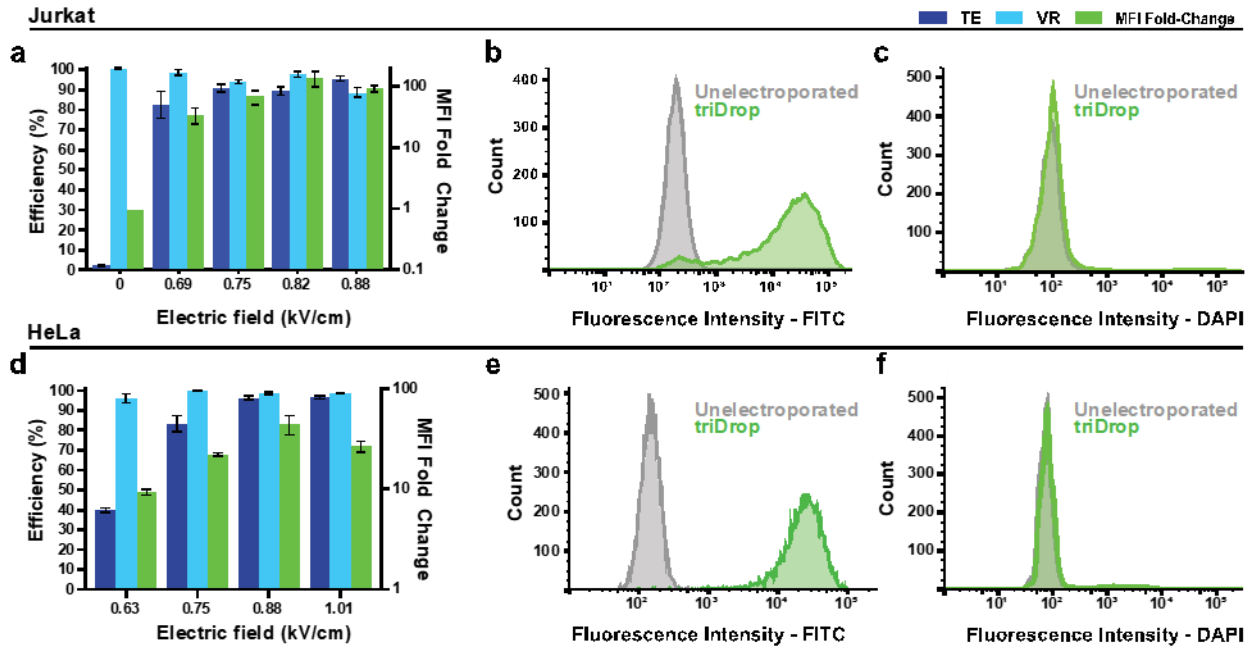


Figure S8: Electroporation parameter optimization for Jurkat and HeLa cells. (a) Voltage optimization using 3, 5 ms pulses on Jurkat cells. (b) FITC fluorescence and (c) DAPI staining comparing an electroperated population (green, 350 V_{DC}) vs a non-electroperated population (grey). (d) Voltage optimization using 3, 10 ms pulses on HeLa cells. (e) FITC fluorescence and (f) DAPI staining comparing an electroperated population (green, 350 V_{DC}) vs a non-electroperated population (grey). All plots with error bars are based on standard error of the mean for n = 3 replicates.

Figure S9: Brightfield and GFP images for immortalized cell lines

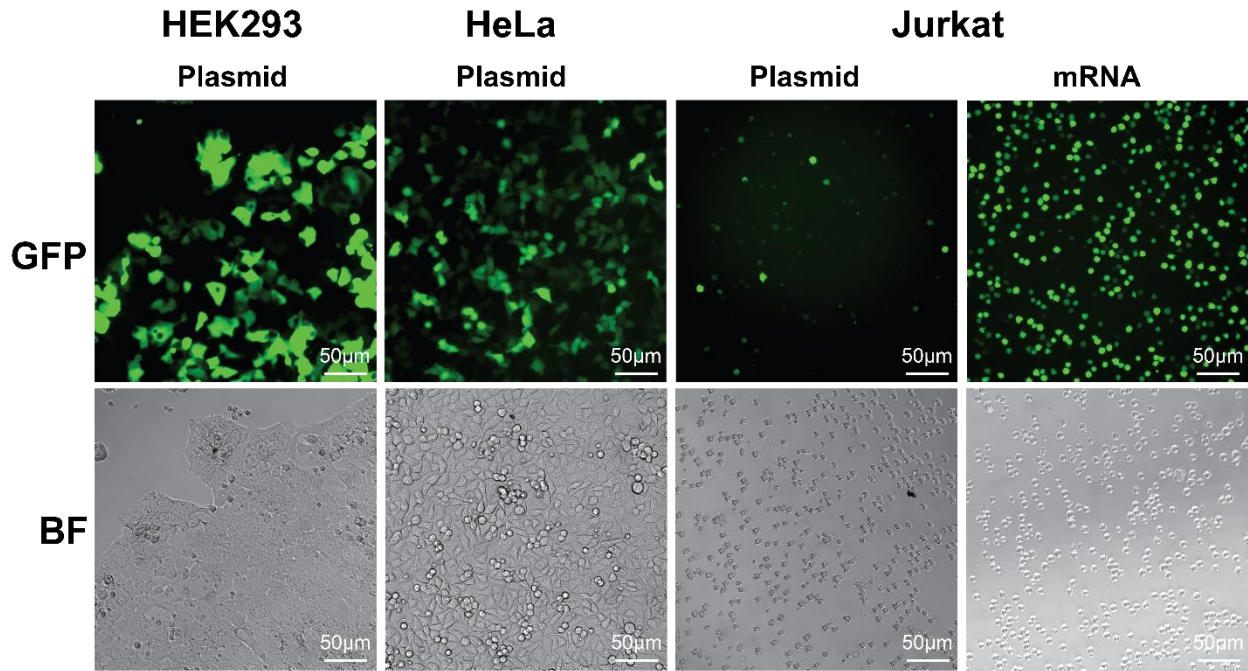


Figure S9: GFP vs brightfield (BF) images for electroporated HEK293, HeLa, and Jurkat cells.

Figure S10: Primary T optimization

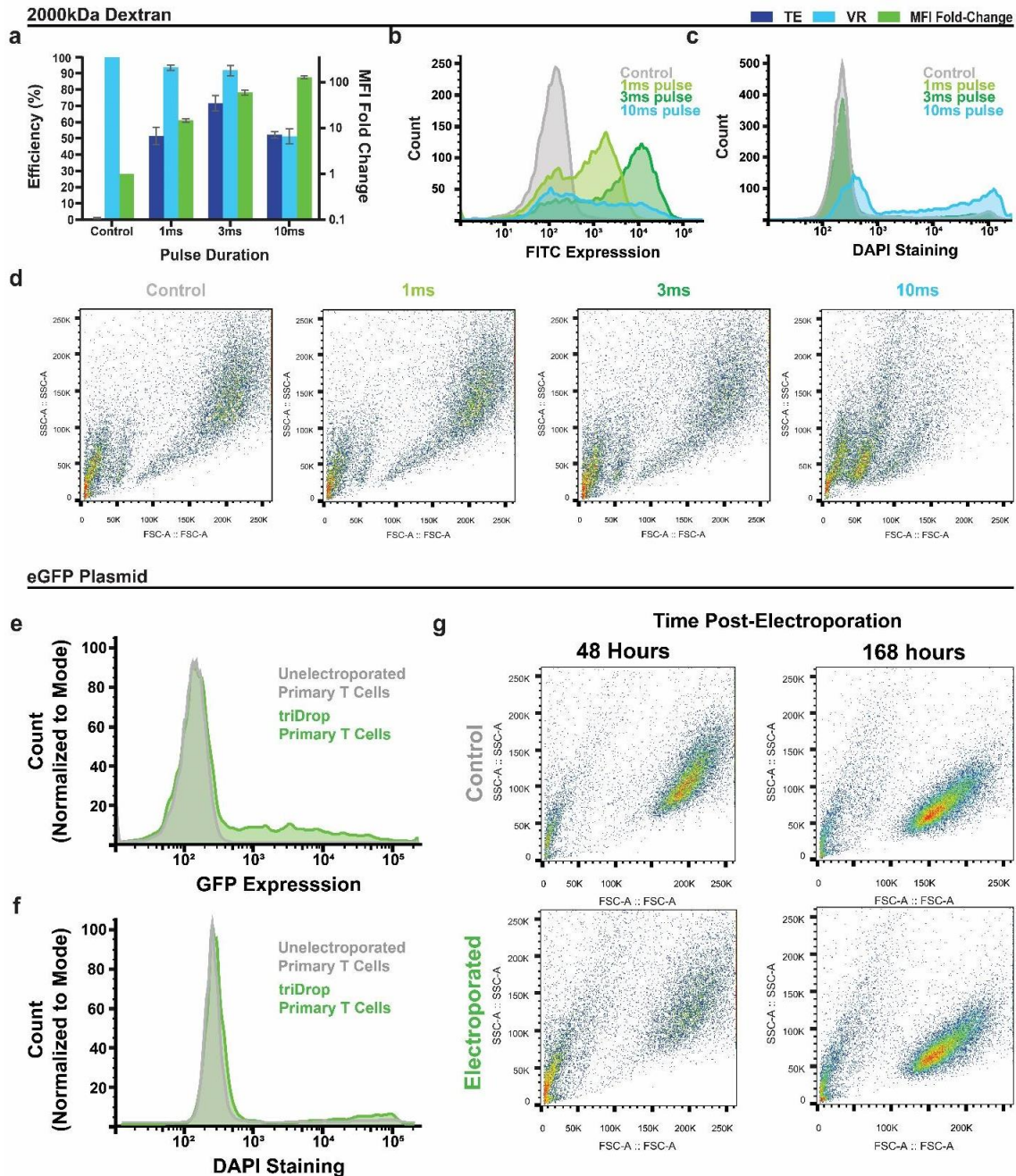


Figure S10: Primary T cell electroporation. (a) TE, VR, and MFI fold-change for primary T cells electroporated with 3, 450VDC pulses either 1ms, 3ms, or 10ms in duration for the insertion of a 2000kDa dextran molecule. (b) FITC fluorescence histograms for 3 different pulse conditions. (c) DAPI staining histograms for 3 different pulse conditions. (d) Side scatter vs. forward scatter plots for a control population and populations electroporated with 3 pulses with a duration of 1 ms, 3 ms, and 10 ms. (e) GFP expression histogram and (f) DAPI staining histogram for primary T cells electroporated with an eGFP plasmid (green) vs a control (grey) 48-hours post electroporation. (g) Side scatter vs. forward scatter for a control population and an electroporated population and control population 48 hours and 168 hours post-electroporation.

Figure S11: Comparison with other recent work – Primary T cell mRNA transfection

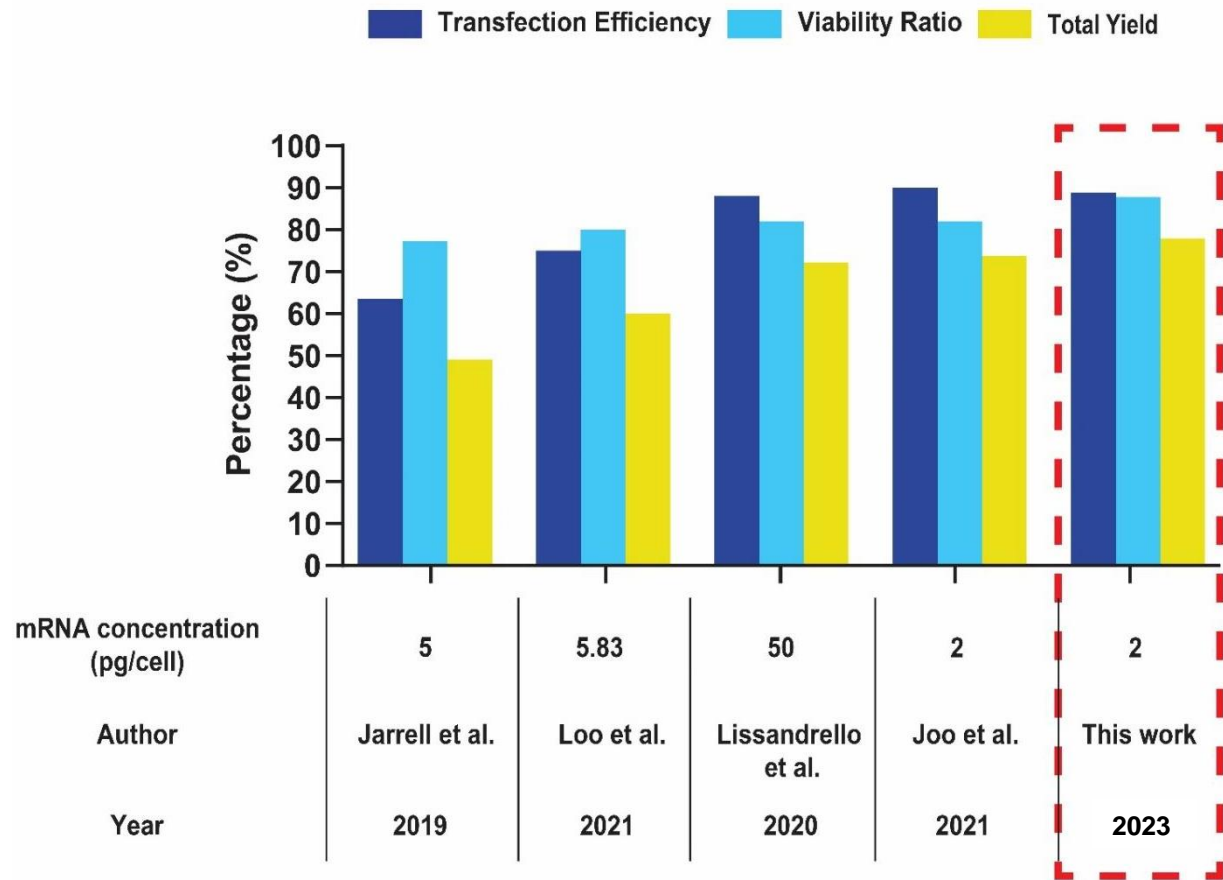


Figure S11: Comparison the transfection efficiency of four recent microfluidic transfection systems with our work for the insertion of eGFP mRNA into primary human T cells.

Figure S12: 5-plex device on-chip operation

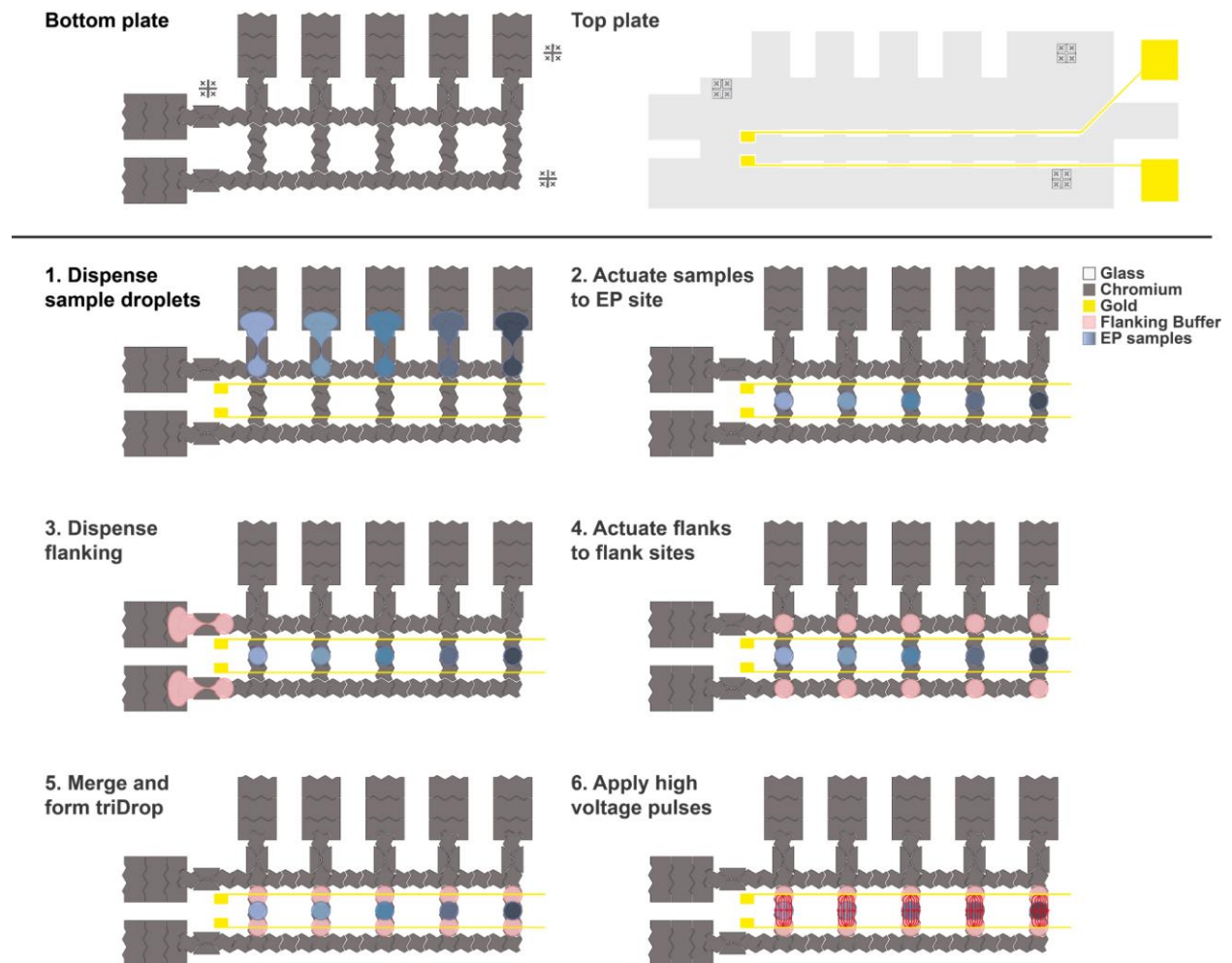


Figure S12: (Top) Electrode designs for bottom and top plates used in the 5-plex device. (Bottom) The five step on-chip automated droplet movements for the formation of five triDrop electroperations in parallel. The different coloured “blue” droplets represent the different guide combinations with primary T-cells that can be dispensed and electroperated with the high conductivity buffer (shown as pink).

Figure S13: multi-gRNA vs single gRNA analysis

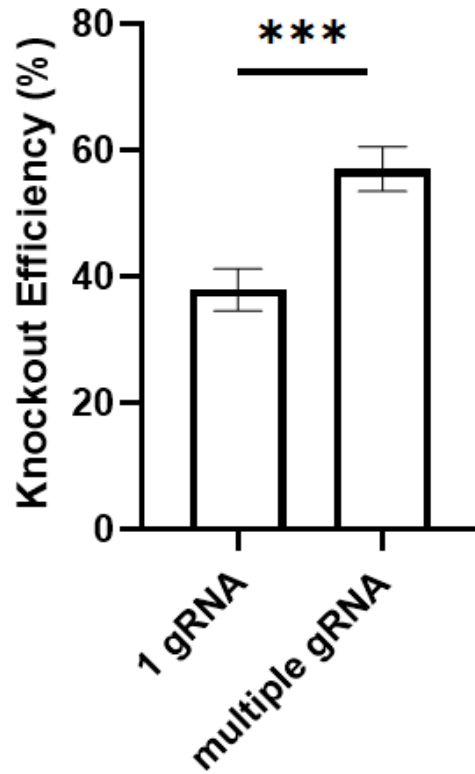


Figure S13: Comparison of primary human T cells electroporated with one gRNA targeting the TRAC-locus vs cells electroporated with multiple gRNAs (combinations of three and four guides). Error bars are based on standard error of the mean for $n = 8$ and $n = 10$ replicates respectively. Statistical analysis was performed using an unpaired T test. $P < 0.001$.

Figure S14: eGFP plasmid map

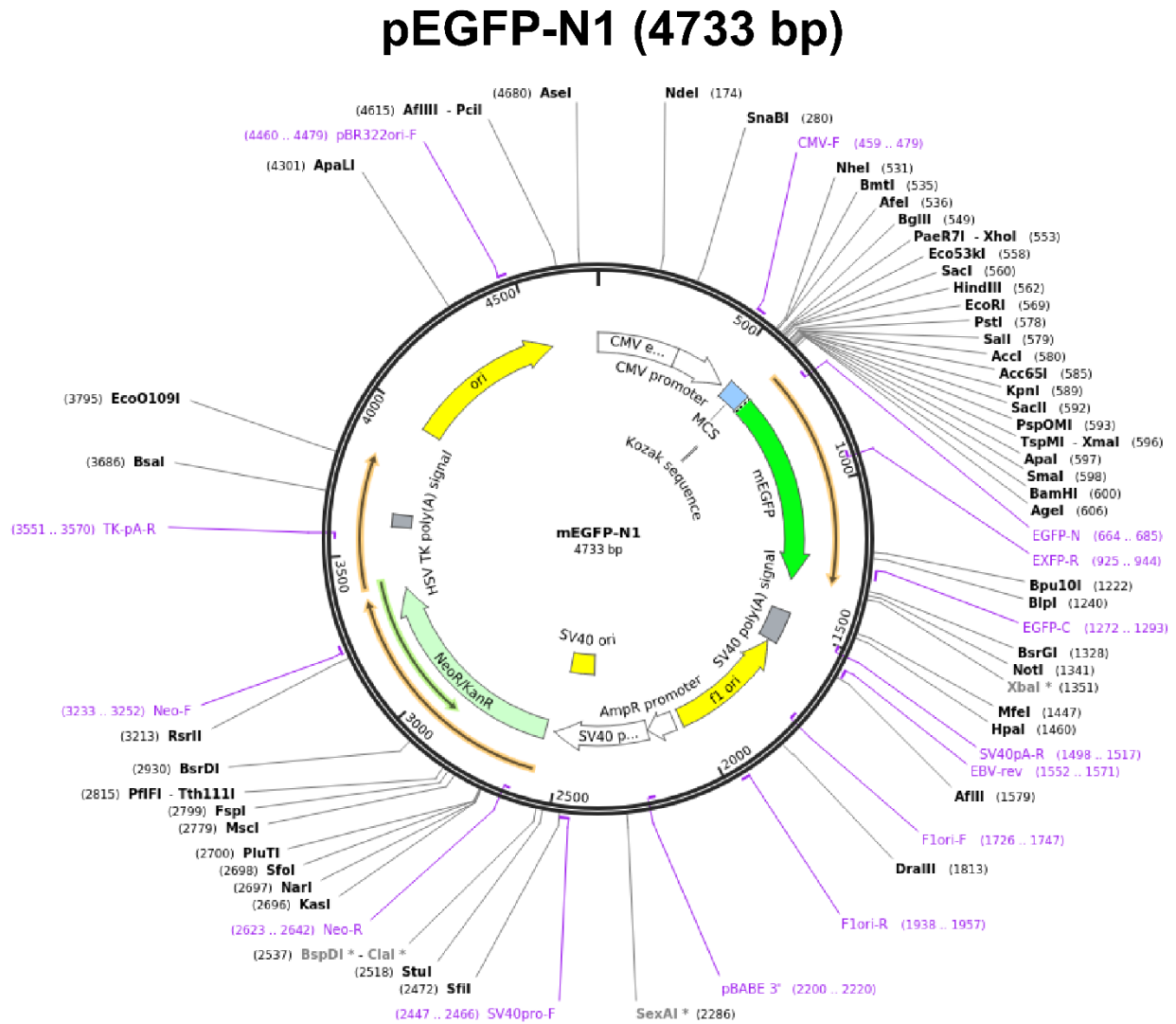


Figure S14: eGFP plasmid map. The plasmid map contains a neomycin or kanamycin resistance marker. The eGFP is driven by a CMV promoter. More information can be found from Addgene (catalog no. 54767).

Figure S15: Fabrication overview

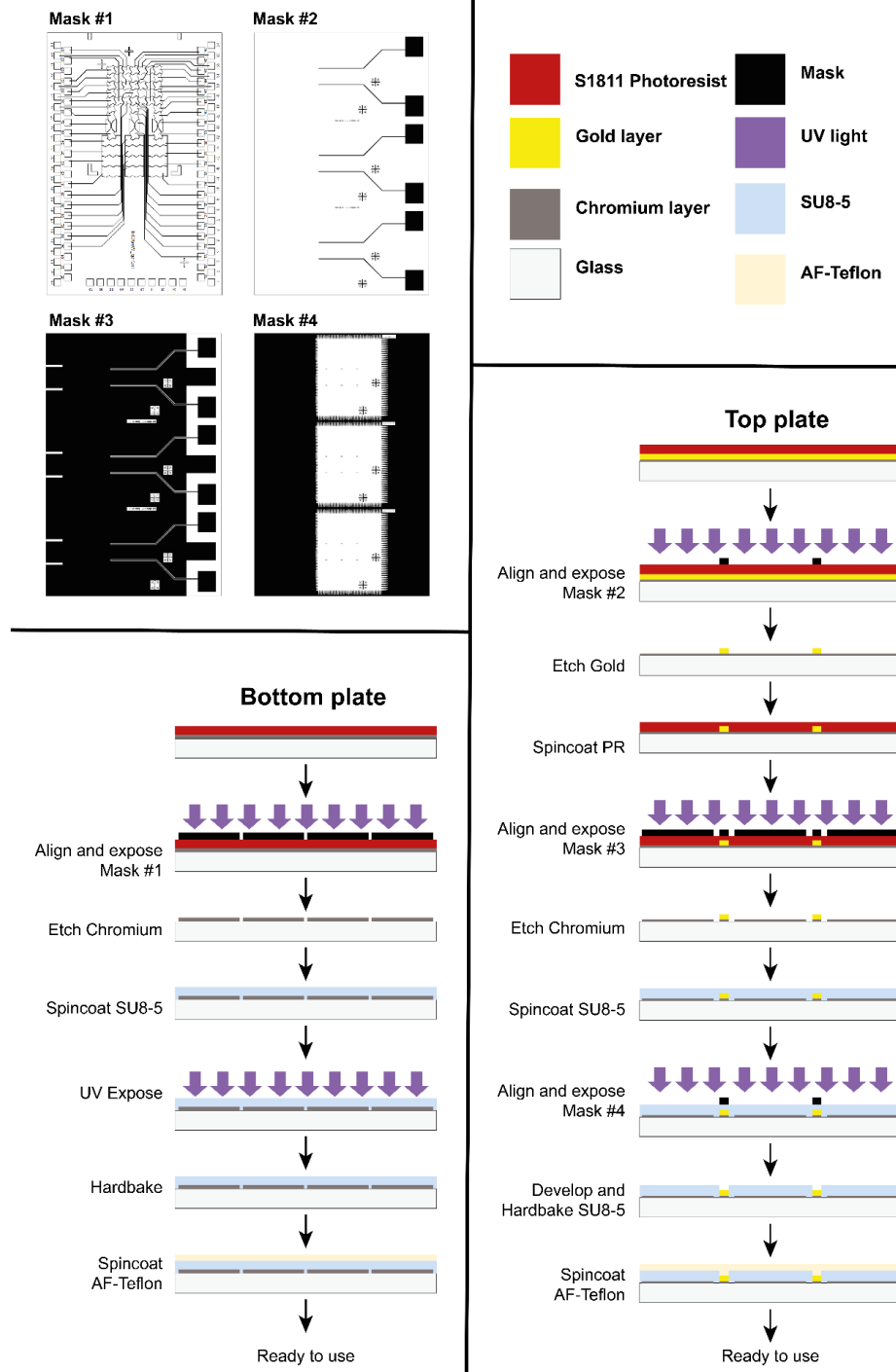


Figure S15: Fabrication procedure shown for the triDrop electroporation digital microfluidic device. The bottom plate shows the general procedure for digital microfluidic bottom plate electrode fabrication. The top-plate shows how to fabricate the gold-lines for electroporating the triDrop structure and to create a semi-transparent top-plate to visualize the droplets. After fabrication, the top-plate is aligned with electrodes on the bottom-plate to ensure the flanking (outside) droplets are touching the gold lines (not shown).

Figure S16: T cell isolation from whole blood

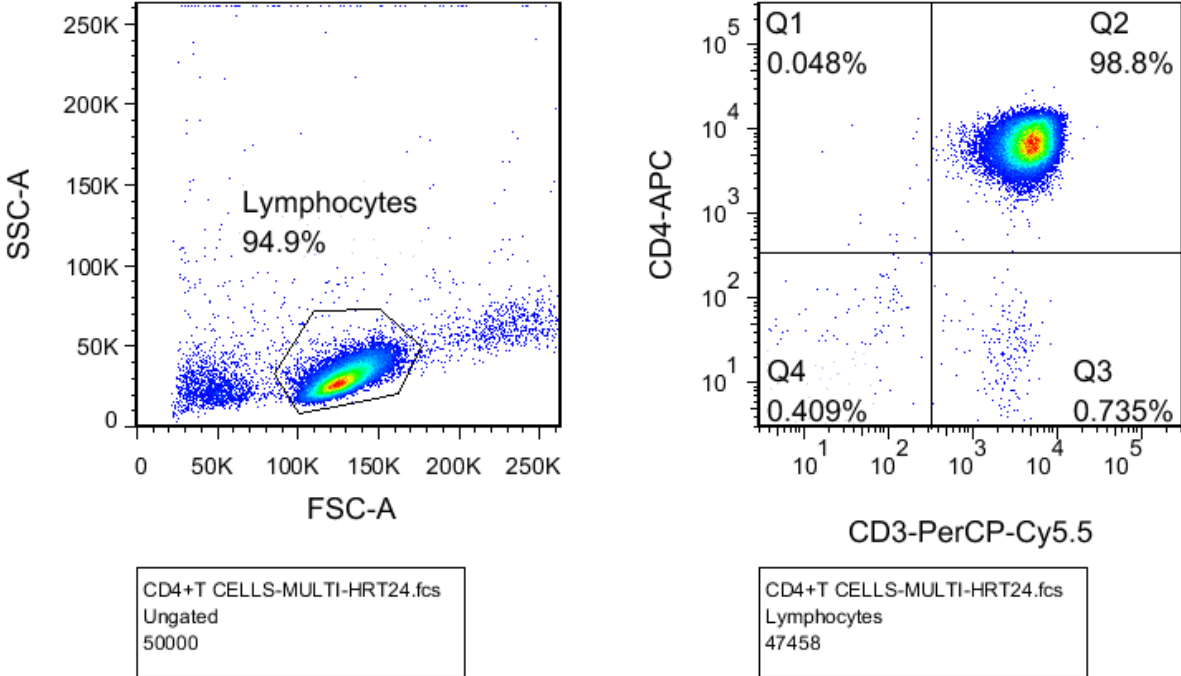


Figure S16: FACS data showing the isolation of CD4+ cell from fresh human blood using the EasySep Human CD4 T cell Isolation kit.

Figure S17: Flow cytometry gating workflow

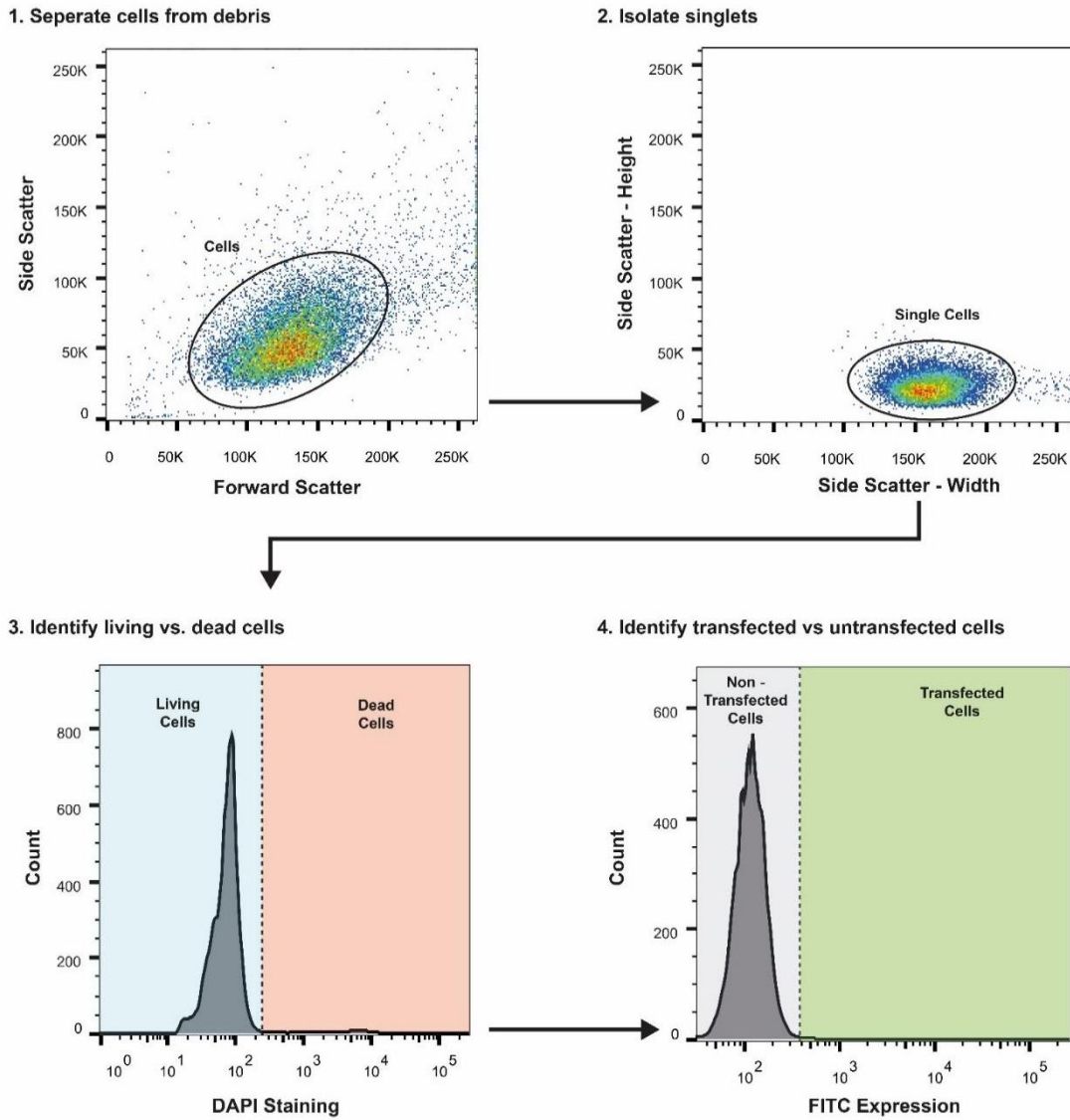


Figure S17: Flow cytometry gating overview. A non-electroporated sample mixed with the prospective payload is used to define gating. First, cells are separated from debris. Next, single cells are isolated from doublets. This is followed by identifying live/dead cells which are determined with DAPI staining. Finally, successfully electroporated living cells are identified.